Optical fiber acoustic sensing multiplexing system based on TDM/SFDM

Jiehui Xie (谢杰辉), Fuyin Wang (王付印), Yao Pan (潘 瑶), Zhengliang Hu (胡正良)*, and Yongming Hu (胡永明)

College of Optoelectronic Science and Engineering, National University of Defense Technology, Changsha 410073, China

**Corresponding author: zheng_liang_hu@163.com*

Received September 10, 2014; accepted November 14, 2014; posted online December 30, 2014

We propose a system of time-division multiplexing (TDM) and spatial frequency-division multiplexing (SFDM). Extrinsic Fabry–Perot interferometric sensors are applied to detect weak acoustic signals. The broadband source is employed, the light from it is modulated by a pulse signal sequence and is efficiently amplified by semiconductor optical amplifiers. Experimental results show that the equivalent noise pressure spectrum level is −97.2 dB re 1 rad/√Hz below 1250 Hz, and the cross talk between two sensors in one TDM channel is −32.7 dB with a cavity length difference of 60 μm. The number of sensors in this multiplexing system can theoretically reach 160.

OCIS codes: 040.1880, 060.2310, 060.4230, 130.6010.
doi: 10.3788/COL201513.010401.

White light interferometers, especially the low-finesse extrinsic Fabry–Perot interferometric (EFPI) sensors, have been widely studied for its outstanding properties such as excellent stability, miniature structure, and absolute measurement[1–6]. An acoustic sensing array based on the miniaturized EFPI sensors can efficiently reduce the size of the multiplexing system and realize the spatial gain of acoustic signals. However, EFPI sensors based on spectra detection have two obvious disadvantages: they are intrinsically difficult to multiplex and they require a broadband source (BBS) with a high light intensity and a broader spectrum range.

To form a multiplexing system, three methods, that is, wavelength-division multiplexing (WDM)[7], frequency-division multiplexing (FDM)[8,9], and time-division multiplexing (TDM)[10] can be separately or jointly applied. For example, a multiplexing system with the combination of coarse WDM and spatial FDM (SFDM) can efficiently take advantage of the light source[11]. However, compared with pure SFDM method, it cannot increase the number of sensors in theory. To further increase sensing channels in the multiplexing system requires another method. Traditionally, TDM excels in increasing the number of sensing channels in the multiplexing system, and the fast fiber Bragg grating analyzer (FBGA, BaySpec Inc.) renders sufficient sampling rate for spectra detection. Meanwhile, SFDM is capable of increasing the number of sensors in a single channel, yet for SFDM with EFPI sensors, the maximum number is limited by the sensors themselves and the light intensity of the BBS[9].

In this letter, we propose and demonstrate a method to increase the number of sensors by combining TDM and SFDM. Semiconductor optical amplifiers (SOAs) are utilized as the pulse modulators for TDM and the optical amplifiers for SFDM, whereas the fast FBGA is used to detect the signal. Compared with other EFPI multiplexing systems based on spectra detection, the proposed system can theoretically multiplex more sensors and respond faster to dynamic signals. Compared with the traditional fiber-optic coherent sensing system, the miniaturized EFPI sensor has a lower equivalent noise pressure spectrum level below 1250 Hz. Experimental results show that our acoustic sensing multiplexing system has a low phase noise and a low cross talk.

The configuration of the multiplexing system is illustrated in Fig. 1. The fast FBGA system serves as a detector array, with a BBS integrated within. This fast FBGA can scan 5000 frames of reflected interference spectra (RIS) per second, which enables the fast FBGA with the capacity of detecting RIS with a high scanning speed. Each spectrum contains 512 pixels in the wavelength domain, ranging from 1506 to 1593 nm. The SOAs are modulated by a pulse signal sequence generated by a function generator. The light from the BBS passing through SOAs is modulated as pulse signals

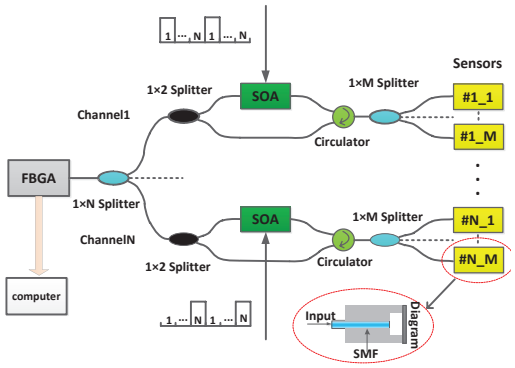

Fig. 1. Schematic diagram of the hybrid TDM/SFDM multiplexing system.

and amplified. Then each light sequence is modulated by the EFPI sensors, and the variations of the cavity lengths represent the intensity of the acoustic pressure. The modulated RIS are sent back into the detector array and then processed by a computer. As shown in the enlarged figure of an EFPI sensor (Ø0.5×1 (cm)), the sensor is formed by a single-mode fiber tip and a gold-coated micro-machined diaphragm. The material of the gold-coated micro-machined diaphragm is the silicon on insulation, and the thickness and radius of the diaphragm are nearly 2 μm and 1 mm.

We demonstrated the feasibility of our method by constructing a two-channel TDM system, with each channel containing two parallel connected EFPI sensors. In a traditional TDM system, the fiber delay line (FDL) is usually utilized to separate the pulse signal sequence. In TDM system, the length of the FDL has to be long enough to separate the pulses between different sensing units. Because the maximum sampling frequency is 5000 Hz, the length of the FDL has to be longer than 20 km. When the number of the TDM channels is N, the length of the FDL is $20(N-1)$ km. However, the length is unacceptable for a miniature sensing system. In our system, we use a function generator to generate a pulse signal sequence with a duty ratio of 50% and a modulation frequency of 2500 Hz, setting a π phase delay between two channels, so that the reflected signals from two channels are separated into an odd and even number sequences.

The novel part of this TDM system is the utilization of SOAs as pulse modulators and optical amplifiers. Compared with most optical switches, the acoustic optical modulators (AOMs) have a higher extinction ratio, and the cross talk between the TDM channels is mainly affected by the extinction ratio of the optical switches. During the preliminary experiments, we used AOMs as pulse modulators, and the maximum intensities of the RIS are shown in Fig. 2(a).

With more sensors added to the system, the light intensity for each sensor will be even more weakened, making the RIS impossible to be demodulated. Therefore, SOAs were applied instead of AOMs, for they can function as pulse modulators while amplifying the light intensity. The maximum intensities of the RIS are shown in Fig. 2(b). Compared with the multiplexing system using AOMs, the system with SOAs achieves a higher light intensity, which is beneficial for the subsequent demodulation and renders the possibility to introduce a large number of fiber optical EFPI sensors when applying SFDM. However, SOAs will introduce higher intensity noises to the RIS, and aggravate the light intensity fluctuation. Therefore, the RIS were filtered by band-pass discrete wavelet transform (DWT) before demodulation.

For a TDM system, it is important to achieve the clock synchronization between pulse modulators and the fast FBGA. The maximum sampling frequency of the fast FBGA may not be 5000 Hz as labeled. To find the actual maximum sampling frequency, the operation of the second channel was stopped. The modulation frequency was firstly set as 2500 Hz (using AOMs as pulse modulators). The waveforms in Fig. 2(a) show a frequency of 10 Hz, which indicates the maximum sampling frequency of the fast FBGA is 4980 Hz instead of 5000 Hz. Therefore, the modulation frequency is reset as 2490 Hz to guarantee the clock synchronization during the second set of experiments with SOAs. Results are depicted in Figs. 3(a) and (b). The spectrum shown in Fig. 3(a) has an excellent waveform, which is advantageous for the subsequent signal processing, whereas the spectrum shown in Fig. 3(b) cannot be used for demodulating because of its low signal-to-noise ratio of the RIS. In other words, the cross talk between different TDM channels can be ignored.

The number of sensors in our SFDM system is mainly determined by two factors. One is the wavelength interval of the sampling point. In our demonstrative system, 1 Hz in the frequency domain after fast Fourier transform corresponds to a cavity length of about 14 μm for RIS. The 512 pixels in each frame limit the cavity length to be less than 3624 μm based on Shannon's

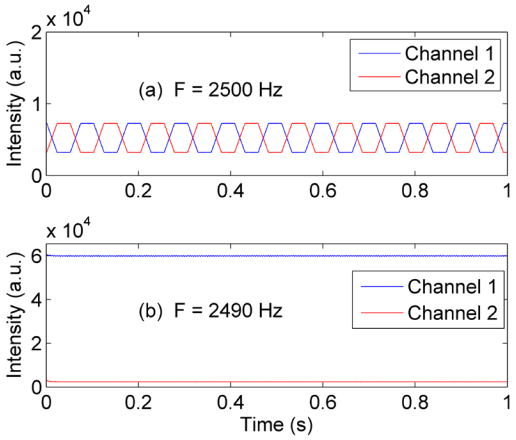

Fig. 2. Light intensities from two sequences. Maximum intensities of the RIS modulated by (a) AOMs and (b) SOAs.

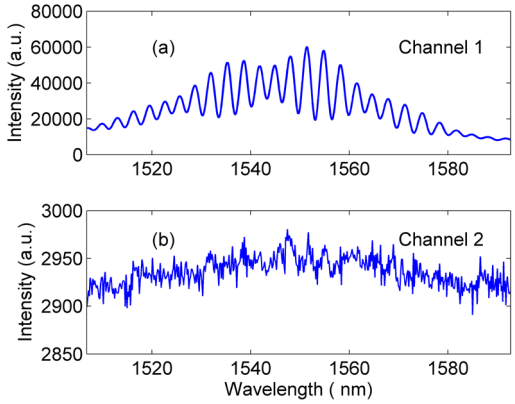

Fig. 3. Waveforms from two sequences. First-frame waveforms of the (a) odd sequence consisting of RIS from two sensors in an on state and (b) even sequence consisting of RIS from two sensors in an off state.

sampling theorem. In practice, a cavity length of less than 1200 μm is better. The other factor is the properties of the sensors. In our system, the reflectivities of the single-mode fiber tip and the diaphragm are approximately 4% and 92%, respectively. The large reflectivity gap allows the cavity lengths of these diaphragm-based EFPI (DEFPI) sensors to be larger than 1 mm[11], which allows more sensors to be introduced into the SFDM system. However, longer cavity results in higher thermal sensitivity of the sensors and lower contrast of RIS. To optimize the performance of our system, we choose a compromised cavity length of 1200 μm.

For a practical SFDM system, choosing the right demodulation method is also important. The RIS are usually interrogated by two typical methods: the discrete gap transform method and the cross-correlation (CC) demodulation method[12–14]. Based on detailed analysis, the latter method has a higher sensitivity to the variations of the cavity length. Owing to the fact that the intensities of acoustic signals are always weak, we chose the CC method as the demodulation method. The CC coefficient can be expressed as

$$\begin{aligned} C(d_j) &= \sum_{j=1}^{M}\sum_{i=1}^{P} I(v_i)\cos\left(\frac{4\pi d_j v_i}{c}+\pi\right) \\ &\approx \frac{v_P - v_1}{2}\sum_{j=1}^{M}\cos\left[\frac{2\pi(d_j-d_i)(v_1+v_P)}{c}+\pi\right] \\ &\quad \operatorname{sinc}\left[\frac{2\pi(d_j-d_i)(v_P-v_1)}{c}\right], \end{aligned} \tag{1}$$

where M is the number of scanning points of the cavity length and P is the number of sampling points in the wavelength domain. λ_i stands for the wavelength of the ith sampling point, c is the light velocity in vacuum, and $v_i = c/\lambda_i$ is the corresponding frequency. $I(v_i)$ is the RIS filtered by DWT and resampled with equal intervals in the frequency domain. The spectrum has the similar expression as the reference function $\cos(4\pi d_j v_i/c + \pi)$. When the CC coefficient C reaches its peak in an allocated range, which is the whole range of the main lobe of the CC coefficient envelope (60 μm in our experiment), the corresponding d_m gives the effective cavity lengths of the EFPI sensors, in which m stands for the number of the sensors in the SFDM system. By scanning cavity lengths, the information within is obtained and demodulated.

Equation (1) states that the main lobe of the CC coefficient envelope is determined by the sinc function. The width of the main lobe is determined by $v_P - v_1$, the light frequency range in one channel. For a certain frequency range, a larger number of channels in the coarse WDM system leads to a narrower frequency range in each channel, resulting in a bigger cavity length interval required among the sensors in a SFDM system thus with fewer sensors in each channel. Hence a system with coarse WDM/SFDM cannot increase the number of sensors compared with the pure SFDM system in theory. On the contrary, TDM method does not sacrifice the light frequency range in each channel to achieve a larger number of sensing channels, thus theoretically the system with TDM/SFDM has the capacity of multiplexing more sensors.

For low-frequency signal detection, the system can potentially be designed as an eight-channel TDM multiplexing system, and each channel may hold more than 20 sensors with cavity lengths varying from 60 to 1200 μm. The maximum sampling frequency of each channel is approximately 625 Hz, which equip the system with the capacity of detecting signals below 300 Hz. Therefore, such optimized design theoretically guarantees a stable and efficient system with more than 160 sensors for low-frequency acoustic detections.

We carried out an experiment with our demonstrative system. Sensors #1_1 and #1_2 were parallel connected in channel one, and sensors #2_1 and #2_2 in channel two. Sensors #1_1 and #2_1 were hung above a loudspeaker, which was driven by a function generator with a frequency of 200 Hz. Sensors #1_2 and #2_2 were placed in another room to avoid the influence of the acoustic signals. The cavity length of each detector was demodulated and is shown in Fig. 4. The sensitivity of each EFPI sensor is nearly 3 nm/Pa[14].

For a multiplexing system, the cross talk among different sensors may severely deteriorate the performance of the system. The cross talk in the same channel is decided by the cavity length differences among the adjacent sensors and the demodulation method. The fluctuations of the cavity lengths shown in Figs. 4(a) and (c) are larger than 10 nm, whereas that of the other two sensors are about 0.4 nm, indicating the low cross talk between adjacent sensors in our system. This is largely owing to the fact that we chose a relatively large cavity length gap in single channel to be around 60 μm.

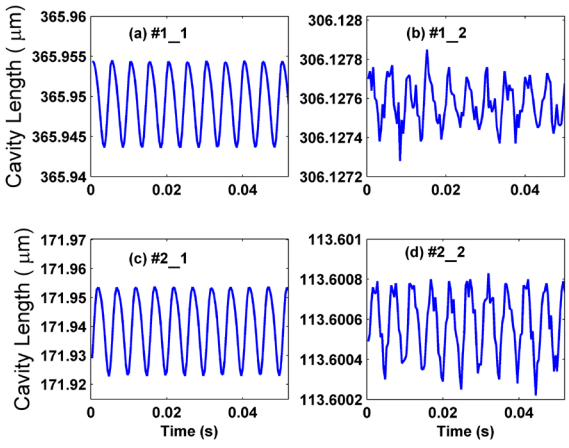

Fig. 4. Acoustic signals demodulated from four sensors in two channels.

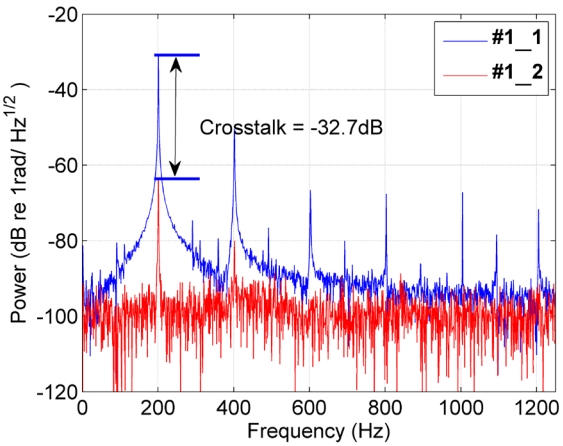

Fig. 5. Two power spectra calculated with phase at wavelength of 1550 nm.

The power spectrum of the system phase noise was calculated with independent variable $\phi = 4\pi d/\lambda$, where d is the cavity length demodulated from the RIS, and the wavelength was $\lambda = 1550$ nm. It can be seen from Fig. 5 that the cross talk between the two DEFPI sensors in channel one is −32.7 dB. The cross talk between other two sensors in channel two was detected as −39 dB. Another important parameter is the equivalent noise pressure spectrum level of the sensor #1_2, which is only −97.2 dB re 1 rad/√Hz when the signal frequency is below 1250 Hz in our system. This outstanding property is benefited from the excellent thermal stability of the miniature structure of the DEFPI sensors, and it enables the DEFPI sensors to detect low-frequency signal with excellent performance. On the contrary, a traditional optical fiber interferometric sensing system usually has a relatively large low-frequency noise, which makes it unsuitable for low-frequency detection.

In conclusion, we propose and demonstrate a method for integrating more sensors in a multiplexing system by combining TDM and SFDM. The utilization of SOAs as pulse modulators rightly made it possible to integrate a larger number of sensors by amplifying the light intensity. The number of the sensors multiplexed in our system can reach 160 theoretically. The cross talk among different channels for TDM can be ignored and the cross talk in one channel among sensors with different cavity lengths is less than −32.7 dB. Experimental results show that the equivalent phase noise of the system is less than −97.2 dB re 1 rad/√Hz below 1250 Hz, a rather appealing property for low-frequency signal detection. Meanwhile, as an absolute demodulation system, it has the capacity to detect two parameters simultaneously. The potential application is to serve as an optic-fiber hydrophone array with the capacity to detect both depth and frequency of the acoustic signal underwater at the same time.

References

1. Y. Jiang, IEEE Photon. Technol. Lett. **20,** 75 (2008).
2. Y. Yu, X. Zhang, Z. Song, Z. Wei, and Z. Meng, Chin. Opt. Lett. **12,** 012301 (2014).
3. F. Xu, L. Lu, W. Lü, and B. Yu, Chin. Opt. Lett. **11,** 082802 (2013).
4. J. Huang, L. Hua, X. Lan, T. Wei, and H. Xiao, Opt Express **15,** 18152 (2013).
5. N. Wang, Y. Zhu, and T. Gong, Chin. Opt. Lett. **11,** 070601 (2013).
6. Y. Ma, X. Qiao, T. Guo, R. Wang, J. Zhang, Y. Weng, Q. Rong, M. Hu, and Z. Feng, Chin. Opt. Lett. **10,** 050603 (2012).
7. J. Yin, T. Liu, J. Jiang, K. Liu, S. Wang, F. Wu, and Z. Ding, Opt. Lett. **19,** 3751 (2013).
8. Y. J. Rao, J. Jiang, and C. X. Zhou, Sens. Actuators A **120,** 354 (2005).
9. J. Jiang, Y. Rao, C. Zhou, and T. Zhu, Acta Phys. Sin. **53,** 2221 (2004).
10. Z. Guo, W. Li, and T. Liu, J. Phys. **276,** 012125 (2011).
11. Y. Rao, C. Zhou, and T. Zhu, IEEE Photon. Technol. Lett. 1**7,** 1259 (2005).
12. Z. Jing and Q. Yu in *Proceedings of the International Society for Optics and Photonics* (2006).
13. C. Belleville and G. Duplain, Opt. Lett. **18,** 78 (1993).
14. J. Xie, F. Wang, Z. Hu, and Y. Hu, Acta Opt. Sin. **34,** s106009 (2014).